AIP Applied Physics Letters

Two-dimensional concentrated-stress low-frequency piezoelectric vibration energy harvesters

Nathan Sharpes, Abdessattar Abdelkefi, and Shashank Priya

Citation: Applied Physics Letters **107**, 093901 (2015); doi: 10.1063/1.4929844
View online: http://dx.doi.org/10.1063/1.4929844
View Table of Contents: http://scitation.aip.org/content/aip/journal/apl/107/9?ver=pdfcov
Published by the AIP Publishing

APPLIED PHYSICS LETTERS **107**, 093901 (2015)

Two-dimensional concentrated-stress low-frequency piezoelectric vibration energy harvesters

Nathan Sharpes,[1] Abdessattar Abdelkefi,[2] and Shashank Priya[1,3]
[1]*Center for Energy Harvesting Materials and Systems (CEHMS), Virginia Tech, Blacksburg, Virginia 24061, USA*
[2]*Department of Mechanical and Aerospace Engineering, New Mexico State University, Las Cruces, New Mexico 88003, USA*
[3]*Bio-Inspired Materials and Devices Laboratory (BMDL), Virginia Tech, Blacksburg, Virginia 24061, USA*

(Received 9 May 2015; accepted 19 August 2015; published online 31 August 2015)

Vibration-based energy harvesters using piezoelectric materials have long made use of the cantilever beam structure. Surmounting the deficiencies in one-dimensional cantilever-based energy harvesters has been a major focus in the literature. In this work, we demonstrate a strategy of using two-dimensional beam shapes to harvest energy from low frequency excitations. A characteristic Zigzag-shaped beam is created to compare against the two proposed two-dimensional beam shapes, all of which occupy a $25.4 \times 25.4\,\mathrm{mm}^2$ area. In addition to maintaining the low-resonance bending frequency, the proposed beam shapes are designed with the goal of realizing a concentrated stress structure, whereby stress in the beam is concentrated in a single area where a piezoelectric layer may be placed, rather than being distributed throughout the beam. It is shown analytically, numerically, and experimentally that one of the proposed harvesters is able to provide significant increase in power production, when the base acceleration is set equal to 0.1 g, with only a minimal change in the resonant frequency compared to the current state-of-the-art Zigzag shape. This is accomplished by eliminating torsional effects, producing a more pure bending motion that is necessary for high electromechanical coupling. In addition, the proposed harvesters have a large effective beam tip whereby large tip mass may be placed while retaining a low-profile, resulting in a low volume harvester and subsequently large power density. © *2015 AIP Publishing LLC*.
[http://dx.doi.org/10.1063/1.4929844]

Piezoelectric energy harvesting has long made use of the cantilever beam due to its ability to transfer a high amount of strain to the attached piezoelectric layers, frequency tunability, and ability to generate closed form analytical modeling.[1–5] However, the shortcomings of the cantilever structure, including narrow bandwidth and the need for large tip mass and/or impractically high aspect ratio to reach low resonance frequencies, have been well established. Surmounting these deficiencies in the one-dimensional cantilever-based vibration energy harvester has been a major focus in the literature, where techniques such as inducing nonlinearity using magnetic coupling configurations,[6–9] axial loading,[8,10] mechanical stoppers,[11,12] varying cross-sectional geometry,[13–15] and employing two-dimensional geometries[16–29] have been examined. In this study, we define a "1D"cantilever as the structure that has constant cross-section, "1.5D" as the structure whose cross-section varies along a single axis, and a "2D"geometry where the cross-section curves or meanders in a plane. It has been shown that 2D beam shapes can outperform 1D beams in terms of power density and low resonance frequency for a given surface area.[16] For this reason, in this study, we pursue a more optimized 2D beam shape, with the goal of increasing electrical power production, while confining the surface area of our harvesters to a $25.4 \times 25.4\,\mathrm{mm}^2$ area. This form factor allows for applications in implantable technologies (e.g., pacemakers) and mobile electronics (e.g., laptop computers and cell phones).

Previous studies have focused on using 2D beam shapes to lower the resonance frequency to match the low frequency sources, using zigzag/meandering,[16–23] spiral,[24–26] and circular arc[27–29] shapes. These geometries are effective at lowering the vibration resonance frequencies by reducing the stiffness of the 2D cantilever structure. However, in the pursuit of low natural frequency, it has been overlooked that lowering beam stiffness is being accomplished by distributing stress throughout the structure, which reduces the beam's ability to stress the piezoelectric element(s) and subsequently decreases the electrical harvested power. Situations may demand this compromise in order to match the harvester's dynamics to the source dynamics, nonetheless, in many other scenarios we need to improve the power density. Here, we provide detailed electrical response of the proposed 2D beam shapes while simultaneously seeking to maintain the low frequency dynamics.

We begin by examining the current art of 2D beam shapes, by defining the Zigzag beam shape shown in the schematic drawing of Fig. 1(a). Since stress transfer from the beam to the piezoelectric material is of principal importance, a finite element stress analysis of the Zigzag beam shape was conducted, as presented in Fig. 1(b), for the first bending mode, found in Fig. 1(c). Fig. 1(b) shows the distributed nature of the stresses in the undeformed Zigzag shape, colored with stress magnitudes resulting from first bending mode vibrations, where warm colors represent tension, cold colors represent compression, with green representing zero stress. Simulations are done in the Stress Analysis environment of Autodesk Inventor Professional 2013. Further details on the finite element analysis can be found in the supplementary material.[33]

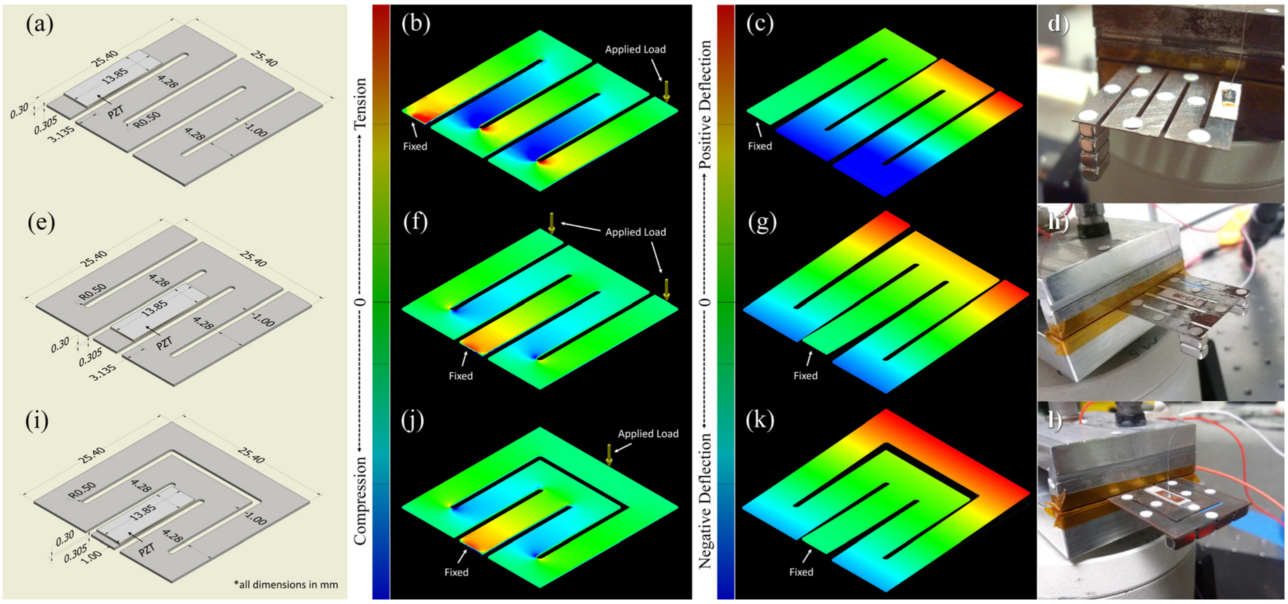

FIG. 1. Dimensioned drawing, finite element stress analysis for first bending mode, first mode shape, and picture of the fabricated device in test setup for Zigzag (a)–(d), Flex (e)–(h), and Elephant (i)–(l) beam shapes, respectively. Coloring of (b), (f), (j) are all with respect to the same arbitrary stress scale, and coloring of (c), (g), (k) are all with respect to the same arbitrary modal displacement scale. (Multimedia view) [URL: http://dx.doi.org/10.1063/1.4929844.1][URL: http://dx.doi.org/10.1063/1.4929844.2]

Distributing stress makes for a more compliant (i.e., less stiff) beam, with low natural frequency. However, this creates a problem when determining where to place the piezoelectric layer(s). If the piezoelectric material is placed throughout the beam, it must be separated and poled in opposition to adjacent segments, as discussed by Berdy *et al.*,[19] due to the alternating sign of stress, as shown in Fig. 1(b). Furthermore, the closer one gets to the free-end of the beam, the lower the magnitude of stress. This results in the situation where each successive segment of piezoelectric becomes less effective and connecting like-poled segments in parallel leads to detrimental charge redistribution and loss of efficiency.[30,31] For this reason, we chose to place the piezoelectric material only on the first segment of our Zigzag harvester, where stress is the highest.

In order to solve the problem of distributed stress in 2D beam shapes, we next seek to create a structure whereby stress is focused onto a single beam segment, upon which the piezoelectric material may be most effectively placed. Another problem to consider is the presence of torsional forces in the Zigzag design. Torsional stresses are not readily harvestable by the flat rectangular profile of these planar 2D beam shapes, due to the resulting orthogonality of electric field to the material polarization and electrodes, and are therefore undesirable.[20,32] Harvester performance should increase if these forces are removed or ideally transformed into bending forces. Torsional forces are also present in spiral and arc-segment based designs.[24–29] Berdy *et al.*[19] have addressed this problem by connecting two Zigzag beam shapes at their free-ends, creating a fixed-fixed configuration. Exploiting symmetry to reduce the onset of torsional forces is valuable; however, a cantilever configuration is a better performing option to a fixed-fixed configuration. Therefore, we introduce the symmetric zigzag cantilever, termed "Flex," and presented in Fig. 1(e). It can be noted that the stress in this design is more concentrated in the first segment near the fixed end, as shown in Fig. 1(f). This is due to the decrease in torsional forces by symmetry, allowing for a more pure bending motion to occur. In this case, rather than placing a unit force on the tip of the beam, as in Fig. 1(b), we place a half unit force on both terminating free ends of the Flex beam shape. The bending motion is also reflected in the mode shape of Fig. 1(g).

With the Flex design, torsional forces are still present due to the two ends being free (i.e., unsupported). It does seem counterintuitive; the merit of the cantilever is the fixed-free configuration, however, in the 2D case, the presence of the free-end not being collinear with the fixed-end creates undesirable torsional effects. It is in the spirit of eliminating free-ends, but somehow maintaining a cantilever-like configuration that we developed the closed-circuit symmetric meandering configuration, termed "Elephant," displayed in Fig. 1(i). From Fig. 1(j), a high concentration of stress can be observed in the first beam segment, due to the optimally pure bending motion of the mode shape, rendered in Fig. 1(k). This is accomplished by joining the meanders on either side of the plane of symmetry at the top of the beam, forming a closed-circuit, whereby torsional effects are forced to cancel out.

To validate the findings of the finite element analysis and quantify the merits of the given concentrated stress structures, experimental investigations were conducted on a series of fabricated test specimens. These test specimens were constructed, according to the dimensions given in Figs. 1(a), 1(e), and 1(i), with the substrate being mild steel and the piezoelectric layer being American Piezoceramics APC850 PZT. Attached to each harvester were also 1.88 g tip masses, consisting of four $6.35 \times 3.175 \times 3.175$ mm neodymium magnets, chosen for their ease of installation and reconfigurability. The fabricated test specimens are shown in Figs. 1(d), 1(h), and 1(l), while the experimental setup is pictured in Fig. 2. Details about the equipment of the experimental setup are found in the supplementary material.[33]

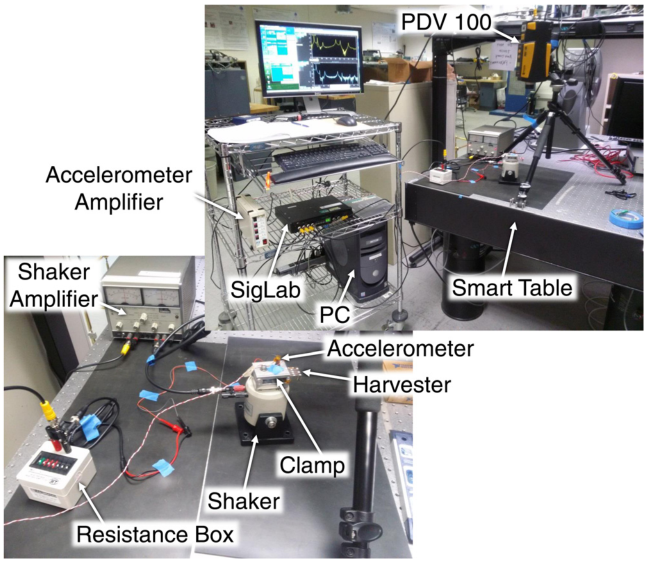

FIG. 2. Experimental setup for characterizing the harvesters fabricated in this study.

The designed harvesters were subjected to varying frequency input (base excitation) and load resistances. Base excitation was held constant at 0.1 g acceleration across all frequencies. Both frequency and resistance were varied manually until maximum values were located. Figs. 3(a)–3(d) show the experimental results for each of the three 2D beam shapes, excited at their first bending frequency, and maximum power/load resistance. The predicted mode shapes have been experimentally validated, discussed in the supplementary material.[33] It follows from Fig. 3(a) that the Zigzag harvester is capable of producing 2.93 μW across 0.75 MΩ at 65.6 Hz. Inspecting Fig. 3(b), we see that the Flex harvester produced 32.2 μW across 1 MΩ at 62.0 Hz base excitation frequency. In both designs, the electromechanical coupling is quite small, as no frequency shift was observable between the short-circuit ($R_L \approx 10^3$ Ω) and open-circuit ($R_L \approx 10^7$ Ω) frequencies. However, for the Elephant harvester, we note a substantial shift between short-circuit and open-circuit frequencies, as well as, a large power output of 81.3 μW across 1 MΩ at 68.125 Hz, as shown in Fig. 3(c). From these findings, we can conclude the merits of the Elephant design, and how it is beneficial towards efficient low-frequency piezoelectric energy harvesting.

It should be noted that while the dimensions of the piezoelectric elements for all three designs are identical, the Elephant has a shorter fixed-end segment, so piezoelectric element is mounted slightly closer to the clamped boundary as compared to the other two designs, giving it access to slightly higher stresses. This bias does not alter the superiority of the Elephant design. Rather, the relative performance of the Zigzag and Flex designs may be marginally closer to that of the Elephant design, had the piezoelectric elements been bonded closer to the clamped boundary.

In addition to the numerical and experimental analyses, a single-degree-of-freedom model is applied to all considered harvesters in order to gain additional understanding of the phenomena involved in their performance. To this end, further testing was conducted, including determining the damping ratio, ζ (via log decrement), and short-/open-circuit frequencies,

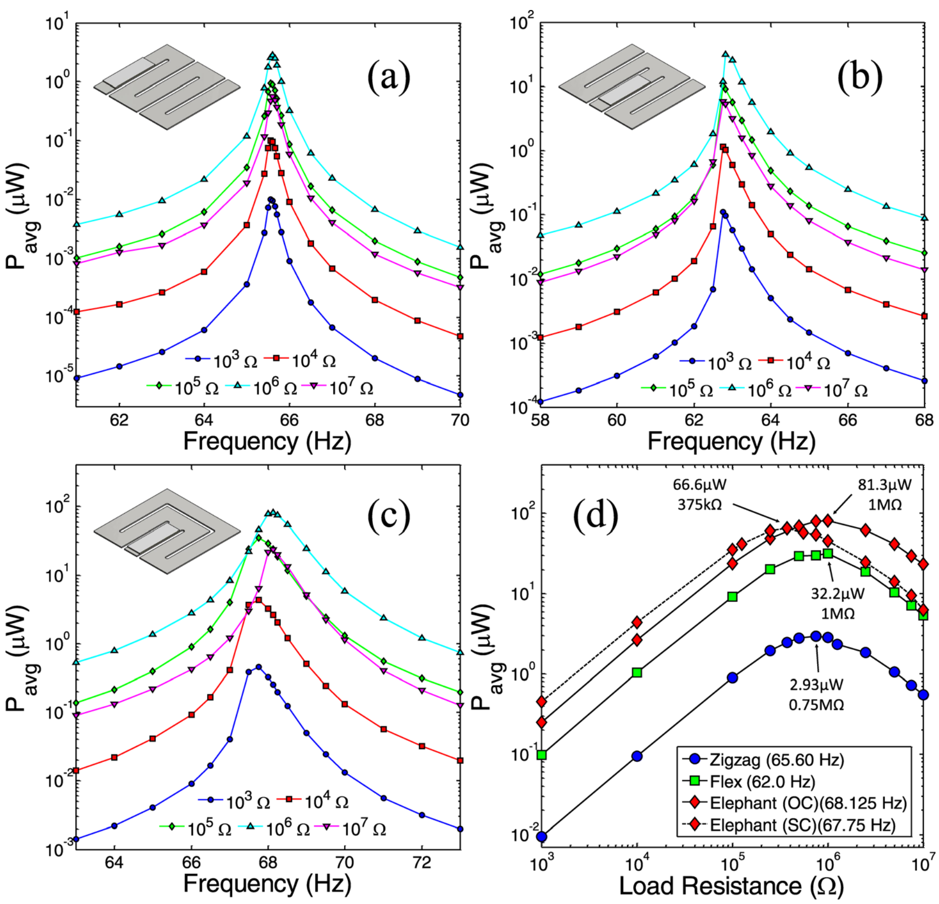

FIG. 3. Experimental results for average power production as a function of frequency and electrical load resistance for (a) Zigzag, (b) Flex, and (c) Elephant configurations, with (d) average power as a function of electrical load resistance at each harvester's respective resonance frequency. All input vibrations were at 0.1 g base acceleration.

TABLE I. Analytical model parameters.

Parameter	Unit	Zigzag	Flex	Elephant
M_b	g	1.51	1.51	1.51
M_{tip}	g	1.88	1.88	1.88
C_P	nF	3.1	3.1	3.1
ζ		0.00611	0.00365	0.00374
ω_{noc}	rad/s	$2\pi(65.6000)$	$2\pi(62.8467)$	$2\pi(68.1250)$
ω_{nsc}	rad/s	$2\pi(65.5888)$	$2\pi(62.7976)$	$2\pi(67.7705)$
Θ	μC/m	20.0515	41.0868	114.8154
a	m/s^2	0.981	0.981	0.981

ω_{nsc} and ω_{noc}, respectively (via high frequency resolution transfer functions). Values used in the model can be found in Table I, where M_b and M_{tip} are the mass of the beam and mass of tip mass, respectively (via A&D EJ-300 scale), C_p is the capacitance of the piezoelectric layer (via Fluke 179 Multimeter), Θ is the electromechanical coupling factor (calculated), and a is the base excitation acceleration. Model derivation and additional parameter measurement procedures are well established in the literature. Thus, detailed explanation of these is given in the supplementary material.[33]

It should be mentioned that the electromechanical coupling coefficient exhibited by the Elephant harvester is larger than its counterparts. This results in a strong increase in the level of the harvested power. Also noteworthy is the large observed damping ratio of the Zigzag design. This, in part, is responsible for the lower observed power and comes from the higher number of segments distant from the fix end, causing more sign changes of the stress, observed in Fig. 1. The Zigzag design has four segments away from the fixed end, while the Flex and Elephant have two, resulting in approximately twice as much damping.

Fig. 4 shows the comparisons between the results of the analytical model and the experimental measurements for the three beam geometries when $R_L = 10^6\ \Omega$. Looking at the coefficient of determination, R^2, there is an excellent fit for the Elephant geometry, a good fit for the Flex geometry, and a poor fit for the Zigzag geometry. This is because the model is suited for describing bending. The influence of torsional effects is not captured in the model, which is the major cause of discrepancy between the model and measurement results. These results further prove how the proposed Elephant 2D beam shape eliminates torsional effects, increasing harvester performance by giving an optimally pure bending motion.

To compare the harvesters proposed in this work to those in the literature, a methodology of comparison is proposed. As the applications and design strategies of piezoelectric energy harvesters are vast, it necessitates a dimensionless parameter comparison. Indeed, those modeling vibration energy harvesters frequently examine their designs with dimensionless parameters; however, this strategy has escaped the comparison of experimental studies. With this impetus, we present the Relative Non-dimensional Harvester Performance Figure of Merit, $\mathcal{S}$, defined as

$$\mathcal{S} = \mathrm{S_P} s_P \mathrm{S_M} s_M S_{BW} s_{BW} S_V s_V, \tag{1}$$

where the upper-case letters indicate relative dimensionless parameters, with lower-case letters being weighting

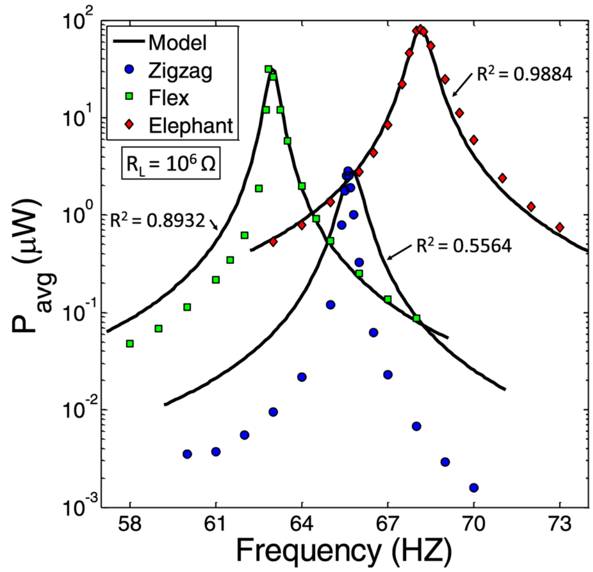

FIG. 4. Comparison of analytical single-degree-of-freedom bending model and experimental results for the case of $10^6\ \Omega$ load resistance.

coefficients, where the sum of the weighting coefficients equals to unity. The individual dimensionless Figures of Merit are defined as

$$\mathrm{S_P} = \frac{P_{avg}\omega_n}{M_{eq}a^2}, \quad S_M = \frac{\sqrt{s_{11}^E \epsilon^T}}{d_{31}}, \quad S_{BW} = \frac{\Delta_{3dB}}{\omega_n}, \quad S_V = \frac{LW}{T^2}, \tag{2}$$

where S_P is the dimensionless power, S_M represents the dimensionless material, S_{BW} denotes the dimensionless band-width, and S_V is the dimensionless volume Figure of Merit, respectively. s_{11}^E is the compliance of the piezoelectric material, or $1/Y_{11}^E$, where Y_{11}^E is the Young's Modulus. ϵ^T is the permittivity of the material, or $K^T\epsilon_0$, where K^T is the relative dielectric constant and ϵ_0 is the permittivity of free space (8.85×10^{-12} F/m). Δ_{3dB} is the half-power bandwidth of the average power versus frequency curve. Finally, L, W, and T are the length, width, and thickness of the harvester, respectively (including all tip masses, materials, circuitry, etc.), as if the harvester was encased in a cuboid. Each dimensionless parameter is made relative (and normalized to unity) by dividing the calculated parameter value for each harvester by the maximum value of each parameter set. Additional dimensionless parameters may be suggested and weighting coefficients adjusted according to individual application needs. For example, if the harvester was to be placed on a large machine vibrating at an unvarying frequency, the weighting coefficients s_{BW} and s_V could be made small. It is also suggested that $s_P = s_M$, since the two are coupled. Compared to the cited experimental works, it is noted, in Fig. 5, that the relative performance of the proposed Elephant harvester is the highest one, where all parameters are given equal weighting, which shows the effectiveness of the designed 2D concentrated stress structures.

In summary, we have shown how the current strategy of using highly compliant 2D beam shapes to harvest energy from low frequency vibrations creates performance reducing torsion. A characteristic Zigzag shaped beam was created to compare against the two proposed 2D beam shapes. The proposed 2D beam shapes, termed as "Flex" and "Elephant,"

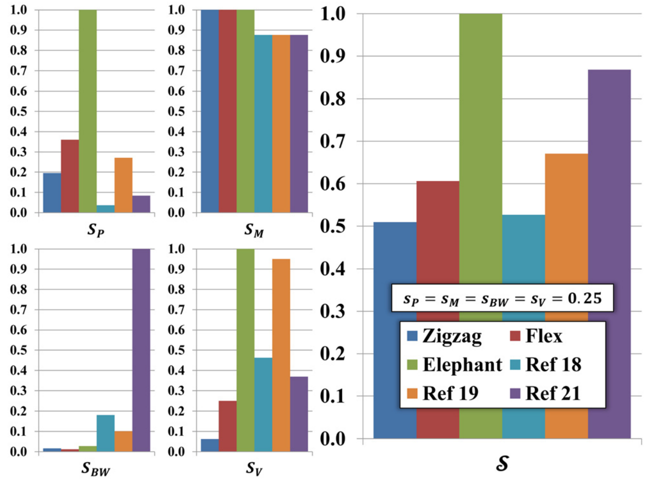

FIG. 5. Relative Non-dimensional Harvester Performance Figure of Merit with equal weighting to all constituent non-dimensional parameters, comparing proposed harvester designs to several literature references.

were created with the goals of realizing a concentrated stress structure, whereby stress in the beam is concentrated in a small area where a piezoelectric layer may be placed, rather than distributed throughout the beam, while also maintaining a low resonance frequency. Through analytical and finite element modeling and experimental measurements, we have shown that through deliberate design, the Elephant harvester was able to provide a significant increase in power production with only a minimal change in resonance frequency, compared to the Zigzag harvester. Moreover, the Elephant harvester has a large effective beam tip whereby large tip mass may be placed while retaining a low-profile, resulting in a low volume harvester, and subsequently large power density. Finally, a strategy for comparing piezoelectric energy harvesters using relative non-dimensional parameters was introduced, where the performance of the Elephant harvester was observed to be higher than that of the considered literature references.

This research was supported through the Samsung Research Program and Office of Naval Research (S.P.) through Center for Energy Harvesting Materials and Systems (CEHMS).

[1]Y. Shu and I. Lien, "Analysis of power output for piezoelectric energy harvesting systems," Smart Mater. Struct. **15**(6), 1499 (2006).
[2]H. A. Sodano, D. J. Inman, and G. Park, "Comparison of piezoelectric energy harvesting devices for recharging batteries," J. Intell. Mater. Syst. Struct. **16**(10), 799–807 (2005).
[3]P. D. Mitcheson, E. M. Yeatman, G. K. Rao, A. S. Holmes, and T. C. Green, "Energy harvesting from human and machine motion for wireless electronic devices," Proc. IEEE **96**(9), 1457–1486 (2008).
[4]S. P. Beeby, M. J. Tudor, and N. M. White, "Energy harvesting vibration sources for microsystems applications," Meas. Sci. Technol. **17**(12), R175 (2006).
[5]K. Najafi, T. Galchev, E. Aktakka, R. Peterson, and J. McCullagh, "Microsystems for energy harvesting," in 16th International Solid-State Sensors, Actuators and Microsystems Conference (TRANSDUCERS) (IEEE 2011).
[6]L. Tang and Y. Yang, "A nonlinear piezoelectric energy harvester with magnetic oscillator," Appl. Phys. Lett. **101**(9), 094102 (2012).
[7]M. A. Karami and D. J. Inman, "Powering pacemakers from heartbeat vibrations using linear and nonlinear energy harvesters," Appl. Phys. Lett. **100**(4), 042901 (2012).
[8]L. Tang, Y. Yang, and C. K. Soh, "Toward broadband vibration-based energy harvesting," J. Intell. Mater. Syst. Struct. **21**(18), 1867–1897 (2010).
[9]A. Abdelkefi and N. Barsallo, "Comparative modeling of low-frequency piezomagnetoelastic energy harvesters," J. Intell. Mater. Syst. Struct. **25**(14), 1771–1785 (2014).
[10]R. Masana and M. F. Daqaq, "Electromechanical modeling and nonlinear analysis of axially loaded energy harvesters," J. Vib. Acoust. **133**(1), 011007 (2011).
[11]H. Liu, C. Lee, T. Kobayashi, C. J. Tay, and C. Quan, "Investigation of a MEMS piezoelectric energy harvester system with a frequency-widened-bandwidth mechanism introduced by mechanical stoppers," Smart Mater. Struct. **21**(3), 035005 (2012).
[12]H. Liu, C. Lee, T. Kobayashi, C. J. Tay, and C. Quan, "Piezoelectric MEMS-based wideband energy harvesting systems using a frequency-up-conversion cantilever stopper," Sens. Actuators, A **186**, 242–248 (2012).
[13]F. Goldschmidtboeing and P. Woias, "Characterization of different beam shapes for piezoelectric energy harvesting," J. Micromech. Microeng. **18**(10), 104013 (2008).
[14]S. Ben Ayed, A. Abdelkefi, F. Najar, and M. R. Hajj, "Design and performance of variable-shaped piezoelectric energy harvesters," J. Intell. Mater. Syst. Struct. **25**(2), 174–186 (2014).
[15]D. Benasciutti, L. Moro, S. Zelenika, and E. Brusa, "Vibration energy scavenging via piezoelectric bimorphs of optimized shapes," Microsyst. Technol. **16**(5), 657–668 (2010).
[16]N. Sharpes, A. Abdelkefi, and S. Priya, "Comparative analysis of one-dimensional and two-dimensional cantilever piezoelectric energy harvesters," Energy Harvesting Syst. **1**(3–4), 209–216 (2014).
[17]M. A. Karami and D. J. Inman, "Electromechanical modeling of the low-frequency zigzag micro-energy harvester," J. Intell. Mater. Syst. Struct. **22**(3), 271–282 (2011).
[18]D. Berdy, B. Jung, J. Rhoads, and D. Peroulis, "Increased-bandwidth, meandering vibration energy harvester," in 16th International Solid-State Sensors, Actuators and Microsystems Conference (TRANSDUCERS) (IEEE 2011).
[19]D. F. Berdy, P. Srisungsitthisunti, B. Jung, X. Xu, J. F. Rhoads, and D. Peroulis, "Low-frequency meandering piezoelectric vibration energy harvester," IEEE Trans. Ultrason. Ferroelectr. Freq. Control **59**(5), 846–858 (2012).
[20]A. M. Karami and D. J. Inman, "Parametric study of zigzag microstructure for vibrational energy harvesting," J. Microelectromech. Syst. **21**(1), 145–160 (2012).
[21]D. F. Berdy, B. Jung, J. F. Rhoads, and D. Peroulis, "Wide-bandwidth, meandering vibration energy harvester with distributed circuit board inertial mass," Sens. Actuators, A **188**, 148–157 (2012).
[22]Y. Hu and Y. Xu, "A wideband vibration energy harvester based on a folded asymmetric gapped cantilever," Appl. Phys. Lett. **104**(5), 053902 (2014).
[23]H. Wu, L. Tang, Y. Yang, and C. K. Soh, "A novel two-degrees-of-freedom piezoelectric energy harvester," J. Intell. Mater. Syst. Struct. **24**(3), 357–368 (2013).
[24]M. A. Karami, B. Yardimoglu, and D. Inman, "Coupled out of plane vibrations of spiral beams," in Proceedings of the 50th AIAA/ASME/ASCE/AHS/ASC Structures, Structural Dynamics, and Materials Conference (2009).
[25]J. A. Brewer, "Low resonant frequency beam design for a piezoelectric energy harvesting device," S.B. thesis (Massachusetts Institute of Technology, 2005), available at http://hdl.handle.net/1721.1/32874.
[26]H. Hu, H. Xue, and Y. Hu, "A spiral-shaped harvester with an improved harvesting element and an adaptive storage circuit," IEEE Trans. Ultrason. Ferroelectr. Freq. Control **54**(6), 1177–1187 (2007).
[27]D. J. Apo, M. Sanghadasa, and S. Priya, "Low frequency arc-based MEMS structures for vibration energy harvesting," in 8th IEEE International Conference on Nano/Micro Engineered and Molecular Systems (NEMS) (IEEE, 2013).
[28]D. J. Apo, M. Sanghadasa, and S. Priya, "Vibration modeling of arc-based cantilevers for energy harvesting applications," Energy Harvesting Syst. **1**(1-2), 57–68 (2014).
[29]D. J. Apo, "Low Frequency Microscale Energy Harvesting," Ph.D. dissertation (Virginia Tech, 2014), available at https://vtechworks.lib.vt.edu//handle/10919/49773.
[30]M. Stewart, P. M. Weaver, and M. Cain, "Charge redistribution in piezoelectric energy harvesters," Appl. Phys. Lett. **100**(7), 073901 (2012).
[31]M. I. Friswell and S. Adhikari, "Sensor shape design for piezoelectric cantilever beams to harvest vibration energy," J. Appl. Phys. **108**(1), 014901 (2010).
[32]A. Abdelkefi, F. Najar, A. Nayfeh, and S. B. Ayed, "An energy harvester using piezoelectric cantilever beams undergoing coupled bending–torsion vibrations," Smart Mater. Struct. **20**(11), 115007 (2011).
[33]See supplementary material at http://dx.doi.org/10.1063/1.4929844 for details about test specimen fabrication, measurement of damping ratio and short-open frequencies, finite element analysis simulations, and analytical model derivation.